THE JOURNAL OF PHYSICAL CHEMISTRY A

ARTICLE

pubs.acs.org/JPCA

Accurate Potential Energy Curve for B_2. Ab Initio Elucidation of the Experimentally Elusive Ground State Rotation-Vibration Spectrum

Laimutis Bytautas,*[,†] Nikita Matsunaga,[‡] Gustavo E. Scuseria,[†,§,∥] and Klaus Ruedenberg[⊥]

[†]Department of Chemistry, Rice University, Houston, Texas 77005, United States

[‡]Department of Chemistry and Biochemistry, Long Island University, Brooklyn, New York 11201, United States

[§]Department of Physics and Astronomy, Rice University, Houston, Texas 77005, United States

[∥]Chemistry Department, Faculty of Science, King Abdulaziz University, Jeddah 21589, Saudi Arabia

[⊥]Department of Chemistry and Ames Laboratory USDOE, Iowa State University, Ames, Iowa 50011, United States

Supporting Information

ABSTRACT: The electron-deficient diatomic boron molecule has long puzzled scientists. As yet, the complete set of bound vibrational energy levels is far from being known, experimentally as well as theoretically. In the present ab initio study, all rotational−vibrational levels of the X $^3\Sigma_g^-$ ground state are determined up to the dissociation limit with near-spectroscopic accuracy (<10 cm^{-1}). Two complete sets of bound vibrational levels for the $^{11}B_2$ and ^{11}B-^{10}B isotopomers, containing 38 and 37 levels, respectively, are reported. The results are based on a highly accurate potential energy curve, which also includes relativistic effects. The calculated set of all vibrational levels of the $^{11}B_2$ isotopomer is compared with the few results derived from experiment [Bredohl, H.; Dubois, I.; Nzohabonayo, P. J. Mol. Spectrosc. 1982, 93, 281; Bredohl, H.; Dubois, I.; Melen, F. J. Mol. Spectrosc. 1987, 121, 128]. Theory agrees with experiment within 4.5 cm^{-1} on average for the four vibrational level spacings that are so far known empirically. In addition, the present theoretical analysis suggests, however, that the transitions from higher electronic states to the ground state vibrational levels v = 12−15 deserve to be reanalyzed. Whereas previous experimental investigators considered them to originate from the v' = 0 vibrational level of the upper state $(2)^3\Sigma_u^-$, the present results make it likely that these transitions originate from a different upper state, namely the v' = 16 or the v' = 17 vibrational level of the $(1)^3\Sigma_u^-$ state. The ground state dissociation energy D_0 is predicted to be 23164 cm^{-1}.

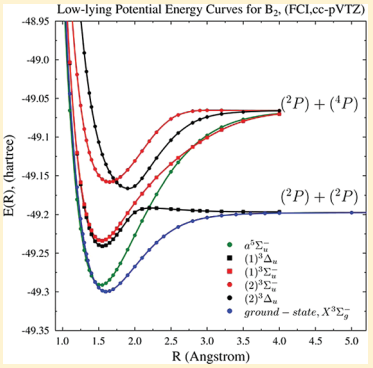

1. INTRODUCTION

Recent developments of efficient ab initio methodologies,[1−20] as well as more powerful spectroscopic techniques,[21,22] have been very productive and a number of challenging problems in physical chemistry can now be resolved. It is well recognized[23−25] that an understanding and interpretation of many experimental observations rely on the quality of ab initio potential energy surface (PES), especially at geometries that are highly distorted from the equilibrium.

A stringent criterion for assessing the quality of a theoretical PES is the capability to yield rotational−vibrational states with high accuracy, either "near-spectroscopic" accuracy of about 10 cm^{-1} or "spectroscopic accuracy" of about 1 cm^{-1}. In many cases, spectroscopic measurements are capable of probing the PES almost all the way to the dissociation limit, e.g., in the molecules H_2, Be_2, LiH, and F_2.[26−30] In other cases however, the intensities of transitions involving highly excited vibrational states, become too weak for detection, as, for example, in the O_2 molecule.[31,32] In such cases, electronic structure theory becomes an especially valuable tool. The regions on a PES representing stretched geometries, which are relevant for highly excited vibrational states, are, however, especially challenging for ab initio studies and, here, methods capable of accurately describing multireference situations are critical[33−37] for attaining near-spectroscopic accuracy. For example, the highest six vibrational levels (above v = 35) of the O_2 molecule were predicted for the first time[38,39] from the potential energy curve calculated with the method of full configuration interaction-correlation energy extrapolation by intrinsic scaling (FCI-CEEIS) method.[40−42] The quality of that method had been validated by the reproduction of the full experimental vibrational spectrum of the F_2 molecule, known up to the dissociation limit, with near-spectroscopic accuracy.[43−46]

Remarkably, among the systems that have puzzled researchers for many years are the small diatomic molecules Be_2 and B_2, containing only eight and ten electrons, respectively. In fact, only in 2009 has the vibrational spectrum of Be_2 been measured,[27] yielding all the bound levels up to the dissociation limit. Similarly, the boron molecule too has been the subject of a long controversy among experimentalists and theorists.[47−63]

Received: November 1, 2011
Revised: December 15, 2011
Published: December 16, 2011

The earliest experimental evidence of a bound B_2 system came from measurements published in 1940 by Douglas and Herzberg.[59] A new band system near 3200 Å in a discharge in helium with a trace of boron trichloride was attributed to B_2 on the basis of arguments related to observed isotope bands and intensity alterations of the fine structure. The authors concluded that this emission system, later called the Douglas−Herzberg (DH) band, resulted from $^3\Sigma_u^- \rightarrow {}^3\Sigma_g^-$ transitions, and that the lower state of this system was the ground state (GS). The $^3\Sigma_g^-$ ground state and the $^3\Sigma_u^-$ excited state are dominated by the configurations $[(\text{core})(\sigma_g2s)^2(\sigma_u2s)^2(\pi_u2p)^2]$ and $[(\text{core})(\sigma_g2s)^2(\sigma_u2s)^1(\pi_u2p)^2(\sigma_g2p)^1]$, respectively. In the 1980s, Bredohl and co-workers[60,61] reinvestigated the emission spectrum of B_2 using high resolution spectroscopy and unambiguously established the triplet character of the ground state. An ESR matrix isolation study by Knight et al.[50] confirmed the $^3\Sigma_g^-$ character of the GS. There has been a considerable amount of theoretical studies concerning the boron molecule as well. The earliest such work was reported by Padgett and Griffing,[47] using a minimal basis set and a self-consistent-field (SCF) level of theory, suggested that the ground state was $^5\Sigma_u^-$. A similar conclusion was reached by Bender and Davidson[48] who used a complete valence configuration interaction method with an extended elliptical orbital basis set. Nonetheless, these authors argued that the DH transition was probably $^3\Sigma_u^- \rightarrow {}^3\Sigma_g^-$. Only in 1978 did calculations by Dupuis and Liu,[49] using a larger basis set and a higher level of electron correlation, finally provide conclusive evidence that the ground state of B_2 is $^3\Sigma_g^-$ and that the DH transition is $(2)^3\Sigma_u^- \rightarrow X\ ^3\Sigma_g^-$. All this information regarding the ground state of the boron molecule notwithstanding, there are many aspects that are still poorly understood. For example, the most accurate and complete experimental data regarding the vibrational energy levels in the ground state of B_2 comes from the studies of Bredohl et al.,[60,61] who deduced the vibrational levels $v = 0$, 1 and $v = 12-15$. But even the highest of these GS levels is still very far from the dissociation limit. Furthermore, in the DH bands, the $0-v''$ transitions corresponding to v'' values from 3 to 11 have not been observed. Thus, 84% of the complete set of bound vibrational energy levels up to the dissociation limit is not known for the ground state of this molecule.

The objective of the present ab initio study is to generate a highly accurate potential energy curve (PEC) for the B_2 molecule, including high-order corrections, and to determine the vibrational energy levels up to the dissociation limit.

2. CALCULATION OF THE GROUND STATE POTENTIAL ENERGY CURVE

The method used to calculate the potential energy curve (PEC) for the ground state of B_2 parallels closely that used for determining the PECs of the F_2 and O_2 molecules.[38,39,43−46] The largest effort was expended on generating near-FCI quality energies in the valence space, ignoring the correlation contribution of the $(1s^2)$ core. The valence space near-FCI results were obtained using the FCI-CEEIS method[40−42] and Dunning's correlation consistent basis sets cc-pVXZ.[64] Extrapolations to the complete basis set (CBS) limits were then performed separately for the zeroth-order energies [at the CASSCF[6/8] level] and the correlation energies [i.e., the differences between the near-FCI and CASSCF[6/8] energies]. Addition of these two quantities yielded the near-FCI/CBS potential energy curve at the nonrelativistic valence-electron-correlation-only limit.

Table 1. Natural Orbital Occupation Numbers for the ROHF and CASSCF[6/8] Wave Functions at Selected Internuclear Distances R for the Ground State $^3\Sigma_g^-$ of the B_2 Molecule

	Molecular Orbitals							
R (Å)	$2\sigma_g$	$2\sigma_u$	$1\pi x_u$	$1\pi y_u$	$3\sigma_g$	$1\pi x_g$	$1\pi y_g$	$3\sigma_u$
	ROHF-Determinant							
	2.0	2.0	1.0	1.0	0.0	0.0	0.0	0.0
	CASSCF [6/8]							
1.55	1.97	1.66	0.97	0.97	0.32	0.05	0.05	0.02
1.60 (eq)[a]	1.96	1.67	0.97	0.97	0.30	0.06	0.06	0.02
2.00	1.94	1.76	0.95	0.95	0.20	0.09	0.09	0.03
3.00	1.90	1.88	0.72	0.72	0.07	0.34	0.34	0.05
6.00	1.89	1.89	0.53	0.53	0.06	0.53	0.53	0.06

[a] Equilibrium geometry.

Subsequent corrections accounting for core correlation, scalar relativity effects and spin−orbit coupling were then added to produce the final PEC. For the purpose of calculating the potential energy curve, the energy of the boron molecule at the internuclear distance of $R = 20$ Å was taken as the separate-atom limit. The GAMESS program suite[65] as well as the MOLPRO package[66] was used by one of us (L.B.) for these ab initio calculations. Details regarding the calculations (i.e., core-correlation effects and relativistic corrections at different points along the GS potential energy curve, as well as a more detailed analysis of the several low-lying excited states) will be reported elsewhere.[67]

2.1. Zero-Order Functions and Energies. As zeroth-order wave function we chose the MCSCF function optimized in the full configuration space generated by the 6 valence electrons using the 8 formal minimal-basis-set valence orbitals, i.e., a wave function of the FORS (full optimized reaction space) type,[68−72] which were subsequently also discussed as CASSCF wave function.[73] This type of full valence space wave function was introduced in the 1970s because it was configurationally unbiased, size-consistent, and properly dissociating. It was also deemed to recover what was then called "non-dynamic" correlation. Novel in-depth studies[9−13,15−18] of this type of correlation have been made more recently under the name static or strong correlation. An early, very accurate FORS = CASSCF[6/8] wave function for B_2[74] recovered the dissociation energy within 16 millihartree. More recently, Peterson, Kendall, and Dunning[75] reported the CBS-extrapolated CASSCF[6/8] as well as the MRCI-SD binding energies based on the suite of correlation-consistent basis sets.

Past experiences and explorations[76−80] have led to the general consensus that MCSCF coefficients or natural orbital[81] occupation numbers (NOONs) in excess of ~0.1 (in addition to the dominant terms in such wave functions) indicate significant multiconfigurational character of physical consequence. Table 1 lists the occupation numbers of the valence NOs of the CASSCF-[6/8] wave function of B_2 at 1.6 Å near the equilibrium distance as well as at other geometries including 6 Å, which is close to dissociation. The $3\sigma_g$ occupation of 0.30 near equilibrium indicates a strong admixture of the configuration $[(\text{core})(\sigma_g2s)^2(\sigma_g2pz)^2(\pi_u2p)^2]$, providing significant σ-bonding, in addition to the dominant $[(\text{core})(\sigma_g2s)^2(\sigma_u2s)^2(\pi_u2p)^2]$ determinant, which contains only π-bonding, as shown by its NO occupation

numbers in Table 1. As expected, upon dissociation the FORS wave function generates mixtures of equal amounts of π_u and π_g occupations that are manifestly required to avoid the appearance of ionic atomic contributions when the atoms separate. The antibonding $3\sigma_u$ orbital plays no significant role along the entire reaction path at this level of approximation.

The calculations of the CASSCF[6/8] energies have been performed with the MOLPRO package[66] for cc-pVQZ, cc-pV5Z, and cc-pV6Z basis sets.[64] The extrapolation of the CASSCF-[6/8] energies to the CBS limit has been done using the data mentioned above via the three-point exponential ansatz as explained in refs 82−84.

2.2. Electron Correlation Energies. The next step was the determination of the residual (dynamic) correlation in the valence space. This was accomplished by calculating the near-FCI energies for the cc-pVTZ and the cc-pVQZ basis sets and subtracting the respective zeroth-order energies discussed in the preceding section. The resulting dynamic correlation energies were then extrapolated to the CBS limit using a two-point X^{-3} formula as described in refs 85 and 86.

The required near-FCI energies were obtained by the CEEIS method. The molecular orbitals were those obtained from the zeroth-order CASSCF[6/8] calculation of the previous section. To reduce the computational effort, the reference function for the CEEIS procedure was, however, taken to be the CI wave function in the full space of six electrons in seven of these orbitals, excluding the ineffective (see section 2.1) $3\sigma_u$ orbital. The latter was then added to the original virtual space. Virtual orbitals of decreasing importance were then obtained by performing a MR-CISD calculation with respect to the "reduced FORS" space CAS[6/7] reference and diagonalizing the *virtual* block of the resulting one-particle density matrix. On the basis of the so constructed reference and virtual space, the CEEIS method[38,43] yielded the near full CI energies. The estimated accuracy of these CEEIS-extrapolated energies is 0.1 millihartree = 22 cm^{-1}.

Finally, the correlation contributions due to the core electron were determined. Although they can be quite large, they change much less along the potential energy curve than the valence shell correlations so that their contribution to the potential energy curve can be calculated using simpler wave functions. The internally contracted icMR-CISD(Q) method[87,88] of the MOLPRO suite[66] was used with Dunning's correlation-consistent cc-pCVQZ and cc-pCV5Z, basis sets, which include tight core functions.[56,89] The procedure is as follows. The molecular orbitals are determined by the CASSCF[6/8] calculation. Then, two icMR-CISD(Q) calculations are done: the first correlating *all ten-electrons*, the second CI correlating only the six valence electrons. The difference between these two energies yields the core correlations for the two basis sets and they were also extrapolated to the CBS limit using the two-point X^{-3} formula. A study by Peterson et al.[56] has shown that the core-correlation effect on the calculated binding energy using the icACPF method differs from a icMRCISD(Q) result by 0.12 kcal/mol for the cc-pCVQZ basis set. Because icACPF wave functions are considered to be a better approximation than icMRCISD(Q) functions due to their approximate size-extensivity, it is reasonable to conjecture that our estimate for the core-correlation effect on the binding energy may have an uncertainty of about 0.1 kcal/mol = 35 cm^{-1}.

Addition of the valence as well as the core correlations to the zeroth-order CASSCF[6/8] energy of section 2.1—*all at the CBS limit*—yielded the near-FCI-CBS energies including all electron correlations. The nonrelativistic potential energy curve was then obtained by subtracting the resulting energies from that at the separate atom limit, which was taken to be reached at 20 Å, about 12.5 times the equilibrium distance. Because the CBS extrapolation may have errors on the order of 0.1 kcal/mol = 35 cm^{-1}, a conservative error bar estimate for our theoretical (all-electron-correlated-CBS) binding energy is 92 cm^{-1}.

2.3. Relativistic Corrections. Two relativistic contributions were added to the nonrelativistic PEC described in the preceding section, viz. the scalar relativistic corrections and the spin−orbit coupling effects.

The former were evaluated by the one-electron Douglas−Kroll (DK) approach,[90] including the transformation to third order (DK3), using the codes due to Nakajima and Hirao[91] and to Fedorov et al.,[92] which are implemented in GAMESS.[65] As discussed in ref 44, these corrections can be adequately determined using a CASSCF[6/8] wave functions and a DK-contracted version of the cc-pVTZ basis sets that have been used in the present study. In-depth comparisons of scalar relativistic effects obtained using DK-contracted basis sets with those obtained using nonrelativistic cc-pVTZ basis sets have been reported by de Jong, Harrison, and Dixon.[93]

The spin−orbit (SO) coupling contributions were evaluated in the two-component approximation by means of the full one-plus two-electron Breit−Pauli operator, using the code of Fedorov and Gordon[94] in GAMESS.[65] The contributions to the ground state result from diagonalizing the Hamiltonian including the SO interaction matrix in CAS-CI basis over a number of states in addition to the ground state. These states and the orbitals from which they are constructed must be chosen judiciously. Because, in the separate atoms as well as in the bonded molecule of B_2, the nonzero spin multiplicities are essentially generated by two electrons using 2p orbitals, the CAS-CI basis was generated by a state-averaged MCSCF calculation for two-electrons in the space of the six valence orbitals that are formed from the 2p orbitals, i.e., the "reduced FORS" space CAS[2/6], where the $2\sigma_g$ and $2\sigma_u$ molecular orbitals are kept as part of the inactive core. The lowest 18 states (singlets and triplets) with $M_S = 0$ were taken into account (M_S denoting the spin projection on the molecular axis). No spatial symmetry restrictions were applied. The basis set was cc-pVTZ. After the CAS-CI basis was determined, the Hamiltonian matrix including the Breit−Pauli terms was formed. The diagonal terms are the spin-free LS-coupled CAS-CI energies. The off-diagonal terms are the spin−orbit couplings between the LS-coupled CAS-CI states. The diagonalization of this Hamiltonian yields the spin-mixed states that are linear combinations of the original CAS-CI states.

The reliability of the method was confirmed by applying it at the near-dissociation limit of $R = 10.0$ Å. The results of the present approach in fact matched the *atomic* calculations for the ^2P state, using the "reduced FORS" space CAS[1/3] wave function generated by the MCSCF-state-averaged calculations for the three states corresponding to singly occupied $2p_x$, $2p_y$, and $2p_z$ orbitals. The molecular calculation at $R = 10$ Å yielded a SO energy lowering of 19.4 cm^{-1}, which coincides with the atomic calculation. Similarly, the difference $[^2P_{3/2} - {}^2P_{1/2}]$ is calculated to be 14.6 cm^{-1} by both approaches and compares well with experimental value of 16 cm^{-1}.[95]

2.4. Full Potential Energy Curve of the $^3\Sigma_g^-$ Ground State. Adding the two relativistic corrections to the nonrelativistic potential described in section 2.2 yielded 33 points on the full potential energy curve. The relative importance of the various corrections for the potential energy curve can be gauged by the

values they have at the equilibrium geometry (1.59 Å), namely:

core correlation energy = −1.97 millihartree

scalar relativistic correction = +0.25 millihartree

spin−orbit coupling effect = +0.09 millihartree

These corrections are the differences for the values at R = 1.59 Å minus the values at R = 20 Å. For increasing values of R, all of them decrease monotonically to zero.

From the 33 ab initio points on the PEC, an analytic PEC curve was obtained by representing it as an expansion in terms of *even-tempered Gaussian functions*, and this analytic expression was then used for calculating the vibration−rotation spectrum to be discussed in section 4.

For many years, expansions in terms of even-tempered Gaussian functions have proven extremely flexible and effective for the construction of radial parts of atomic basis orbitals.[96,97] More recently, calculations on the molecules F_2 and O_2[39,45] have shown these expansions also to be highly effective for generating accurate expressions of diatomic potential energy curves by least-mean-squares fitting to relatively few accurate data points. This capability is presumably due to the fact that they combine an unbiased high flexibility with the constraints intrinsic to globally coherent analytic, i.e., everywhere infinitely differentiable functions. In contrast, PEC representations that lack such a global analytic coherence require a correspondingly greater density of individual data points to generate evenly accurate fits. This is in particular the case for fitting in terms of local cubic splines, which would require an order of magnitude closer spacing of data points to yield a good quality curve. In view of the considerable effort that goes into the calculation of the individual ab initio energies on the potential energy surface, the advantages of the even-tempered representations in the context of ab initio work are manifest. For some PECs, eventempered *exponential* expansions[98] may be better suited than even-tempered Gaussian expansions.

The long-range decay of potential energy curves is typically of the $(1/R^n)$ type of course and accurate treatments of long-range potentials in terms of sums of inverse-power terms have, e.g., been developed by Le Roy, Coxon, Pashov, Tiemann, and co-workers (see, e.g., refs 99−101). The exact form of this dependence in a specific molecule cannot always be predicted a priori, however. For instance, the first accurate ab initio calculation of the transition from short-range to long-range R-dependence, namely for the $^1\Sigma_g^+$ ground state of F_2[46], showed the long-range tail to be *very* different from all previous expectations.[102] Also, in the recent experimental study of the spectrum of the Be_2 molecule by Merritt, Bondybey, and Heaven[27] (see also ref 103), a formula *with* a specific preformulated built-in long-range inverse-power-polynomial tail yielded a *worse* fit to the experimental data than a formula *without* such tail. Fortunately, our work on F_2[46] showed that the transition to the inverse power regime occurs only when the value $V(R)$ of the PEC has become too small to be of quantitative consequence in the context of the present analysis. (For all nonzero values of J, the potential including the centrifugal term decays as R^{-2} so that, for them, the long-range decay of the pure vibrational component is irrelevant.)

The even-tempered expansion of the $^3\Sigma_g^-$ ground state of B_2 is given in Table 2. The parameters listed in that table were obtained by a linear regression fit to the 33 ab initio energies. (Possibly, sequential rounding and refitting according to Le Roy[104] could make these numerical data even more compact by removing unnecessary digits without loss of accuracy.) Table 3 lists the actual ab initio PEC values together with the values produced by the even-tempered fit. The maximum absolute deviation is seen to be 0.069 millihartree; the mean absolute deviation is 0.029 millihartree. Thus, this analytic PEC recovers the ab initio data with a deviation that is an order-of-magnitude smaller than the maximal error *estimated* for the individual ab initio calculations. We believe that the merging of the information from all 33 data points may render the analytic PEC a better approximation to the true PEC than the individual raw ab initio data and that this is one reason that the vibrational energies obtained for F_2 and O_2 deviated only by less than 15 cm^{-1} (on the average) from the experimental spectrum. Table 3 also provides information regarding the total energies obtained for the B_2 ground state.

Table 2. Analytic Representation of the Full Ground State Potential Energy Curve of B_2 in Terms of Even-Tempered Gaussian Functions

$$V(R) = \sum_{k=0}^{7} a_k e^{-\alpha\beta^k R^2}$$

parameters[a]	values
α	0.166
β	1.5368
a_0	8.23987249
a_1	−107.15781150
a_2	303.54772065
a_3	−1668.82025703
a_4	2015.42869563
a_5	−353.81494323
a_6	2257.70466507
a_7	3915.44790772

[a] Units: α, $Å^{-2}$; a_k, millihartree; β, dimensionless.

The equilibrium distance for B_2 is found to be R = 1.5886 Å. The experimental[59] value is 1.590 Å. At the equilibrium distance, the full PEC has the value −107.923 millihartree with an estimated error bar of 0.42 millihartree, leaving also room for possible deviations due to the transition from the exponential to an expected inverse power decay at large distances.[46] Taking into account the theoretical zero-point energy of 2.381 millihartree, which is determined in section 4 below, yields the dissociation energy D_0 = 105.54 ± 0.42 millihartree = 66.23 ± 0.25 kcal/mol. The experimental estimates for D_0 in the literature, all of thermochemical and mass-spectrometric origin, have relatively large error bars: 65.49 ± 5.52 kcal/mol,[105] 69.60 ± 2.32 kcal/mol,[106] and 68.00 ± 13.81 kcal/mol.[107]

3. CALCULATION OF THE POTENTIAL ENERGY CURVES OF FIVE EXCITED STATES

Dupuis and Liu[49] had conclusively shown that the experimental vibration−rotation spectrum of Douglas and Herzberg[59] involve transitions from the second excited $^3\Sigma_u^-$ state (i.e., $2^3\Sigma_u^-$) to the $^3\Sigma_g^-$ ground state. Subsequently, this was also presumed to be the case for the spectrum found by Bredohl and co-workers.[60,61] Later, however, questions were raised[54] regarding this interpretation. To probe these questions, theoretical information regarding the relevant excited states is required.

Table 3. Quality of the Fit of the Analytic Expansion of Table 2 to the ab Initio PEC Values of B_2 (Energies in Millihartree)

R, Å	$V(R)_{FIT}$	$V(R)_{ab\ initio}$	$[V(R)_{FIT} - V(R)_{ab\ initio}]$
1.10	133.281	133.296	−0.015
1.20	17.535	17.468	0.067
1.25	−21.429	−21.431	0.002
1.28	−40.072	−40.050	−0.022
1.30	−50.786	−50.755	−0.031
1.33	−64.558	−64.528	−0.031
1.35	−72.355	−72.329	−0.026
1.40	−87.650	−87.644	−0.006
1.45	−97.918	−97.939	0.021
1.50	−104.181	−104.218	0.037
1.55	−107.272	−107.305	0.033
1.59	−107.922	−107.944	0.022
1.60	−107.870	−107.889	0.019
1.65	−106.529	−106.522	−0.007
1.70	−103.700	−103.669	−0.031
1.80	−94.994	−94.936	−0.057
1.90	−83.987	−83.947	−0.040
2.00	−72.185	−72.194	0.009
2.10	−60.587	−60.637	0.050
2.20	−49.822	−49.875	0.053
2.30	−40.247	−40.267	0.019
2.40	−32.020	−31.986	−0.033
2.60	−19.562	−19.488	−0.074
2.80	−11.631	−11.617	−0.013
3.00	−6.914	−6.958	0.044
3.20	−4.215	−4.266	0.051
3.40	−2.670	−2.684	0.014
3.60	−1.749	−1.729	−0.019
3.80	−1.162	−1.132	−0.030
4.00	−0.765	−0.750	−0.015
5.00	−0.036	−0.088	0.052
6.00	0.010	−0.058	0.069
20.00	0.000	0.000[a]	0.000

[a] For the near-FCI/CBS valence-correlation-only level of theory, the energy of B_2 at this point is $E(20\ Å) = -49.205699$ hartree; i.e., this value does not include the effects associated with the core correlation and relativistic effects.

Because the $2^3\Sigma_u^-$ state is the fifth state in the corresponding irreducible representation A_u of the point group D_{2h} with $M_S = 1$, which is the one used in the working programs, we determined the potential energy curves for the five lowest states of A_u symmetry with $M_S = 1$. Among these five states there are four triplet states and one quintet state. In view of the small magnitudes of the corrections discussed at the end of section 2.3 and because, in addition, electron transitions are *differences* between electronic states, it was considered adequate to calculate the excited states at the valence near-FCI level with cc-pVTZ basis sets.

To this end, we developed the following *generalization of the CEEIS method to the simultaneous calculation of several states*. A *five-state-averaged* MCSCF calculation in the full valence space, i.e., CASSCF[6/8], was performed for $M_S = 1$ and the A_u irrep of D_{2h}. That is, the orbitals were optimized on the basis of the state-average of the lowest five states of the full [6/8] CI matrix in A_u symmetry for $M_S = 1$. The ineffective $3\sigma_u$ was again moved from the reference to the virtual orbital space. Virtual orbitals of decreasing importance were then obtained by performing a MR-CISD calculations with respect to the lowest ^3A_u state in the reduced CAS[6/7] reference space and diagonalizing the virtual block of the resulting one-particle density matrix. Using increasing numbers of these virtual orbitals, successive CI calculations including single, double, triple, and quadruple excitations with respect to the CAS[6/7] reference space then yielded the required energies for each of the five lowest states. Note that, at each level of these calculations, the five states remain mutually orthogonal. On the basis of these data, the CEEIS *extrapolation to the near-FCI energy of each state* was then readily performed. Higher than quadruple excitations were found to be negligible. This multistate generalization of the CEEIS method proved entirely successful.

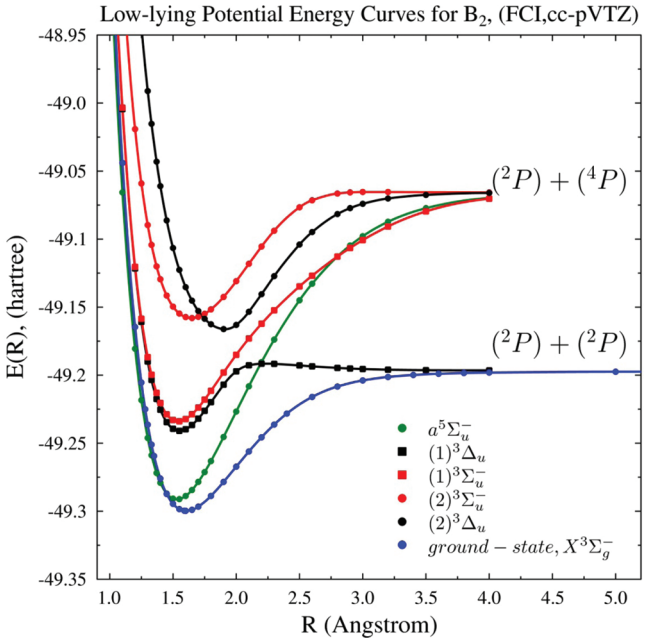

Figure 1. Potential energy curves of the B_2 molecule for the ground state (irreducible representation B_{1g} in D_{2h}) and the five lowest states of the irreducible representation A_u in D_{2h}. (FCI/cc-pVTZ calculations, see text).

The resulting five states have the symmetries $^5\Sigma_u^-$, $^3\Delta_u$, $^3\Sigma_u^-$, $^3\Sigma_u^-$, $^3\Delta_u$. The corresponding potential energy curves, as obtained at the described valence-FCI level with the cc-pVTZ bases, are exhibited in Figure 1. The figure also includes the PEC of the $^3\Sigma_g^-$ ground state, calculated at the same level of correlation approximation.

For the two states $1^3\Sigma_u^-$ and $2^3\Sigma_u^-$, which will be of interest below, as well as for the ground state, all at the (valence near-FCI/cc-pVTZ) level, analytic representations of the PECs in terms of even-tempered Gaussian functions[97] were obtained by a least-mean-squares linear regression fit to 33 points (for the ground state) and to 29 points (for the excited states) that represent ab initio energies. Tables S1−S6 of the Supporting Information list the data for these analytic PEC representations as well as for the ab initio and fitted energy values at these points.

dx.doi.org/10.1021/jp210473e |J. Phys. Chem. A 2012, 116, 1717–1729

Table 4. Comparative Assessment of Power Expansions of Rotational Energies of the isotopomer $^{11}B_2$[a]

	rotational constants (cm^{-1})			energies (cm^{-1}) and deviations[b] (10^{-4} cm^{-1})			
v	B_v	$-D_v$	H_v	$F(J=1)$	$F(J=4)$	$F(J=7)$[c]	$F(J=10)$
0				**2.4128**	**24.1252**	**67.5375**	**132.6244**
	1.2063910	−6.4996 (−6)		0.0004	0.006	0.02	−0.02
	1.2063910	−6.5012 (−6)	1.546 (−11)	0.0003	0.0003	−0.009	−0.02
	1.2063861	−6.5002 (−6)	1.018 (−11)	−0.1	−1	−3	−5
20				**1.7430**	**17.4265**	**48.7760**	**95.7567**
	0.8715034	−8.9823 (−6)		0.002	−0.004	−0.06	0.2
	0.8715032	−8.9745 (−6)	−7.319 (−11)	0.0002	−0.0005	−0.006	0.02
	0.8715006	−8.9734 (−6)	−8.217 (−11)	−0.05	−0.5	−1	−3
30				**1.1788**	**11.7817**	**32.9507**	**64.6125**
	0.5894591	−1.8829 (−5)		0.02	−0.04	−0.7	2
	0.5894577	−1.8730 (−5)	−9.339 (−10)	−0.0001	0.0004	−0.001	0.006
	0.5894578	−1.8730 (−5)	−9.183 (−10)	0.003	0.03	0.09	0.3
37				**0.5216**	**5.1990**	**14.4580**	**28.0976**
	0.2609387	−4.9729 (−5)		0.5	−0.7	−14	39
	0.2609107	−4.7755 (−5)	−1.852 (−8)	−0.01	0.1	−0.06	0.8
	0.2609146	−4.7870 (−5)	−1.585 (−8)	0.06	0.6	3	27
38				**0.3936**	**3.8967**	**8.0738**[c]	*d*
	0.1970539	−1.1342 (−4)		1	−10	23[c]	*d*
	0.1969826	−1.0198 (−4)	−2.626 (−7)	−0.05	0.2	0.7[c]	*d*
	0.1969942	−1.0351 (−4)	−1.825 (−7)	0.1	3	38[c]	*d*

[a] Each section contains data for a given value of v, as labeled in column 1: Columns 2−4 list the constants for the power expansions in eq 2. Columns 5−8 list the exact rotational energies $F(J)$ as well as the deviations of the approximated $F(J)$ values from the exact $F(J)$ values for four values of J. In each section, the first line lists the exact rotational energy values $F(J)$. The second line contains the constants and deviations obtained by the quadratic fit to the exact levels. The third line contains the constants and deviations obtained by the cubic fit to the exact levels. The fourth line contains the constants and deviations obtained by perturbation theory.[109,110] [b] $[F(J,\text{approximate}) - F(J,\text{from DVR})]$. [c] For $v = 38$ and $J = 7$ the rotational level $E_{v,J}$ = lies slightly above the dissociation limit. The deviations listed refer therefore to J=6 rather than $J = 7$. [d] For $v = 38$, the levels for $J > 7$ lie above the dissociation limit.

4. ROTATIONAL−VIBRATIONAL ENERGY LEVELS

4.1. Method. The ro-vibrational energy levels $E_{v,J}$, where v and J are the vibrational and rotational quantum numbers respectively, were obtained from the nuclear Schrödinger equation with the analytic representation of the potential energy curves in terms of even-tempered Gaussians as discussed in sections 2.4 and 3. The solutions were found by the discrete variable representation (DVR) procedure,[108] the details of the implementation being identical to those described in our earlier studies.[39,45]

The high-lying vibrational states are well converged in our DVR procedure. The first grid point R_{in} and the last grid point R_{out} as well as the grid spacing ΔR of the even-spaced points in between were obtained by monitoring the vibrational energy levels as functions of these three parameters. The end points R_{in} and R_{out} were chosen such that the wave function of the highest energy level has effectively converged to zero at these end points. To this end, the values of $R_{in} = 1$ Bohr, $R_{out} = 25$ Bohr and $\Delta R = 0.04$ Bohr were found to be sufficient. Although none of the calculated energy levels exhibited any further change when the number of grid points exceeded 400, in all calculations 600 grid points were used.

The DVR method is also applicable to the Hamiltonians that include nonvanishing rotational energies, i.e., with the potential $[V(R) + (\hbar^2/2\mu)J(J+1)/R^2]$ where $J > 0$, as long as the resulting eigenvalue $E_{v,J}$ does not lie above the dissociation limit of the electronic state being considered and its wave function does not become oscillatory at larger distances. In the ground state of $^{11}B_2$ it was found that for $J = 0$ (i.e., the pure vibrational spectrum) as well as for $J = 1-6$, the vibrational levels 0−38 lie below the dissociation limit. For $J = 7-10$, only the vibrational levels $v = 0-37$ lie below that limit. The level for ($v = 38, J = 7$) seems to lie slightly above this limit. Rotational Hamiltonians with $J > 10$ were not examined.

The rotation-vibration energy levels were then reorganized in the standard form[106]

$$E_{v,J} = V_{min} + E_v + F_v(J) \quad (1)$$

where V_{min} is the minimum value of the potential $V(R)$ at the equilibrium distance R_{eq} and the E_v are pure vibrational levels; i.e., by definition all rotational terms $F_v(J)$ vanish for $J = 0$. They were furthermore represented by the standard expansions

$$F_v(J) = B_v[J(J+1)] - D_v[J(J+1)]^2 + H_v[J(J+1)]^3 + \ldots \quad (2)$$

whose coefficients B_v, D_v, and H_v were determined by linear regressions using the expression

$$[F_v(J)/J(J+1)] \approx B_v - D_v[J(J+1)] + H_v[J(J+1)]^2 \quad (3)$$

In accordance with the above-mentioned findings, the least-mean-squares fittings were based on the levels $J = 1-10$ in the case of $v = 0-37$. But for $v = 38$ the fitting was based on the levels $J = 1-6$. (In the case of the isotopomer ^{11}B-^{10}B, the fitting for $v = 37$ was based on the levels $J = 1-7$).

The quality of eq 2 is assessed in Table 4 for a number of representative vibrational energy levels. For each of these, the

Table 5. Theoretical Vibrational Levels and Rotational Constants for the Ground State of $^{11}B_2$[a]

v	$E_v - E_0$ (cm^{-1})	E_v[b] (cm^{-1})	$E_v - E_{v-1}$ (cm^{-1})	B_v[c] (cm^{-1})	B_v(fit)[d] (cm^{-1})	D_v(fit)[d] (10^{-6} cm^{-1})
0	0.00	522.52		1.20639	1.20639	6.499
1	1031.93	1554.44	1031.93	1.19202	1.19202	6.517
2	2046.35	2568.87	1014.43	1.17754	1.17754	6.541
3	3043.08	3565.59	996.72	1.16293	1.16293	6.571
4	4021.88	4544.39	978.80	1.14816	1.14816	6.608
5	4982.51	5505.03	960.64	1.13324	1.13324	6.652
6	5924.73	6447.25	942.22	1.11812	1.11812	6.703
7	6848.25	7370.77	923.52	1.10280	1.10280	6.764
8	7752.78	8275.30	904.53	1.08725	1.08725	6.833
9	8638.00	9160.52	885.22	1.07145	1.07145	6.913
10	9503.57	10026.09	865.57	1.05537	1.05537	7.004
11	10349.13	10871.65	845.56	1.03898	1.03898	7.108
12	11174.28	11696.79	825.15	1.02226	1.02226	7.226
13	11978.60	12501.11	804.32	1.00518	1.00518	7.359
14	12761.64	13284.15	783.04	0.98768	0.98768	7.511
15	13522.91	14045.42	761.27	0.96974	0.96974	7.683
16	14261.89	14784.40	738.98	0.95131	0.95131	7.878
17	14978.01	15500.53	716.12	0.93233	0.93233	8.101
18	15670.66	16193.18	692.65	0.91275	0.91275	8.355
19	16339.18	16861.70	668.52	0.89250	0.89250	8.647
20	16982.85	17505.37	643.67	0.87150	0.87150	8.982
21	17600.88	18123.39	618.03	0.84967	0.84967	9.371
22	18192.41	18714.92	591.53	0.82689	0.82689	9.822
23	18756.49	19279.01	564.09	0.80304	0.80304	10.35
24	19292.11	19814.62	535.61	0.77799	0.77799	10.98
25	19798.10	20320.62	505.99	0.75154	0.75154	11.72
26	20273.22	20795.73	475.12	0.72349	0.72349	12.62
27	20716.06	21238.58	442.85	0.69359	0.69359	13.72
28	21125.11	21647.63	409.05	0.66153	0.66154	15.06
29	21498.70	22021.22	373.59	0.62696	0.62696	16.74
30	21835.08	22357.59	336.37	0.58946	0.58946	18.83
31	22132.47	22654.98	297.39	0.54864	0.54864	21.43
32	22389.37	22911.89	256.91	0.50428	0.50428	24.57
33	22605.03	23127.55	215.66	0.45665	0.45665	28.05
34	22780.26	23302.78	175.23	0.40704	0.40705	31.38
35	22918.26	23440.77	138.00	0.35771	0.35772	34.23
36	23024.09	23546.61	105.83	0.30994	0.30995	38.24
37	23102.27	23624.78	78.18	0.26091	0.26094	49.73
38	23153.51	23676.03	51.25	0.19699	0.19705	113.42

[a] R(eq) = 1.5886 Å, V(eq) = −23686.30 cm^{-1}. [b] Vibrational energy levels E_v with respect to the bottom of PEC. [c] Calculated as expectation value (see ref 45, eq 14). [d] Calculated by linear regression, see eq 3.

first line lists the $F(J)$ values obtained by the DVR calculation. The second line lists the constants obtained by LMSQ fitting when the last term on the RHS of eqs 2 and 3 is omitted. The third line lists the constants when this term is included. For each choice of constants the resulting deviations of the respective approximations from the exact values of $F_v(J)$ are given for the values J = 1, 4, 7, 10, except in the case of v = 38 where the deviations for J = 1, 4, 6 are given for the aforementioned reasons.

Listed in addition (fourth line for each v) are also the constants and the corresponding deviations that result from the perturbation approach of Hutson[109] and Tellinghuisen,[110] which is often used by experimental spectroscopists, taken to second order. All constants from the perturbation approach were obtained by Le Roy with his program LEVEL.[111] The authors thank Professor Le Roy for kindly making this information available to them. It was noted that the perturbation expansion taken to seventh order does not seem to converge for v = 38 and J = 9 and 10, i.e., for levels in the continuum above the dissociation limit.

Table 4 shows that the agreement between the various types of rotational constants is very close and that they all reproduce the actual energies within a few thousandths of a cm^{-1}. The cubic fit to $F(J)$ yields the best constants, recovering the energies better than 10^{-4} cm^{-1}. The constants from the first three terms of the perturbation theory yield consistently the largest error, which is due to the omission of the higher-order terms. In the case of $\{v = 38, J = 6\}$ for instance, including the terms up to seventh order will

Table 6. Theoretical Vibrational Levels and Rotational Constants for the Ground State of ^{11}B-^{10}B

v	$E_v - E_0$ (cm^{-1})	E_v[a] (cm^{-1})	$E_v - E_{v-1}$ (cm^{-1})	B_v[b] (cm^{-1})	B_v(fit)[c] (cm^{-1})	D_v(fit)[c] (10^{-6} cm^{-1})
0	0.00	535.30		1.26623	1.26623	7.162
1	1056.85	1592.15	1056.85	1.25077	1.25077	7.183
2	2095.32	2630.62	1038.47	1.23519	1.23519	7.210
3	3115.19	3650.49	1019.87	1.21946	1.21946	7.244
4	4116.22	4651.52	1001.03	1.20357	1.20357	7.286
5	5098.16	5633.46	981.94	1.18748	1.18749	7.337
6	6060.72	6596.03	962.56	1.17120	1.17120	7.397
7	7003.61	7538.92	942.89	1.15468	1.15468	7.467
8	7926.51	8461.81	922.89	1.13790	1.13790	7.548
9	8829.06	9364.36	902.55	1.12084	1.12084	7.640
10	9710.90	10246.20	881.84	1.10347	1.10347	7.747
11	10571.62	11106.92	860.72	1.08575	1.08575	7.868
12	11410.80	11946.10	839.18	1.06766	1.06766	8.006
13	12227.97	12763.27	817.17	1.04914	1.04914	8.163
14	13022.63	13557.94	794.67	1.03017	1.03017	8.342
15	13794.26	14329.56	771.62	1.01068	1.01068	8.546
16	14542.26	15077.56	748.00	0.99063	0.99063	8.778
17	15266.01	15801.31	723.75	0.96996	0.96996	9.044
18	15964.83	16500.14	698.82	0.94859	0.94859	9.348
19	16637.99	17173.29	673.15	0.92645	0.92645	9.700
20	17284.66	17819.97	646.68	0.90343	0.90343	10.11
21	17903.98	18439.28	619.32	0.87944	0.87944	10.58
22	18494.97	19030.27	590.99	0.85434	0.85434	11.14
23	19056.56	19591.87	561.59	0.82797	0.82797	11.79
24	19587.58	20122.89	531.02	0.80017	0.80017	12.58
25	20086.73	20622.04	499.15	0.77069	0.77069	13.52
26	20552.57	21087.88	465.84	0.73929	0.73929	14.67
27	20983.51	21518.81	430.93	0.70563	0.70563	16.09
28	21377.80	21913.10	394.29	0.66933	0.66933	17.85
29	21733.58	22268.88	355.78	0.62994	0.62994	20.07
30	22048.94	22584.24	315.36	0.58702	0.58702	22.85
31	22322.15	22857.45	273.21	0.54022	0.54022	26.25
32	22552.14	23087.44	229.99	0.48967	0.48967	30.14
33	22739.35	23274.65	187.21	0.43655	0.43656	33.99
34	22886.69	23422.00	147.35	0.38328	0.38329	37.26
35	22999.42	23534.72	112.72	0.33170	0.33171	41.39
36	23082.63	23617.94	83.22	0.27947	0.27950	52.74
37	23137.79	23673.09	55.15	0.21368	0.21378	111.9

[a] Vibrational energy levels E_v with respect to the bottom of PEC. [b] Calculated as expectation value (see ref 45, eq 14). [c] Calculated by linear regression, see eq 3.

reduce deviation from ~0.004 to ~0.0003 cm^{-1}. In as much as perturbation expansions are not unique, it is not surprising that direct fitting to the data produces constants that generate the fewest terms for a given level of accuracy.

4.2. Results. The results of the calculations for the ro-vibrational spectra of the ground states of the two isotopomers $^{11}B_2$ and ^{11}B-^{10}B are reported in Tables 5 and 6, respectively. The vibrational levels are listed in columns 2−4, the rotational constants are listed in columns 5−7. The vibrational terms are given as the actual energy levels with respect to the bottom of the PEC in column 3 and as the levels with respect to the zero point energy (ZPE) in column 2. Also given are the energy level spacings, i.e., the separations between adjacent levels (column 4). The rotational constants B_v from the linear regression fits of eq 3 are listed in column 6. Column 5 also gives the values obtained for the B_v as expectation values, i.e., the first term in the perturbation expansion.[109,110] The values of D_v are listed in column 7. They are those obtained from the regression fits to the *linear* form of eq 3. For the isotopomer $^{11}B_2$, the theoretical vibrational energy levels can be compared with the experimental levels that can be reconstructed from the experimental spectroscopic constants given by Douglas and Herzberg[59] and by Bredohl, Dubois, and Nzohabonayo.[60] This comparison is shown in Table 7 for v = 0−3 because the experimental data correspond only to low v values. It is evident that the agreement between the theory (column-2) and both experiments (columns 3 and 4) is very good. A comparison for all vibrational levels up to v = 14 is shown in Table S7 of the Supporting Information.

The vibrational spectra were also calculated for the (valence near-FCI/cc-pVTZ based) PECs of the three states X $^3\Sigma_g^-$,

Table 7. Comparison of the Ground State Vibrational Energy Levels for Low Values of v Obtained from the High-Accuracy ab Initio Calculations with the Levels Deduced from the Experimental Spectroscopic Constants of Bredohl et al.[60] and Douglas and Herzberg[59] (Energy unit: cm^{-1})[a]

	E_v		
v	this study	Bredohl et al.[60]	Douglas-Herzberg[59]
0	522.52	523.88	523.3
1	1554.44	1556.74	1555.8
2	2568.87	2569.72	2569.5
3	3565.59	3562.82	3564.4
	$E_v - E_{v-1}$		
v	this study	Bredohl et al.[60]	Douglas-Herzberg[59]
1	1031.92	1032.86	1032.5
2	1014.43	1012.98	1013.7
3	996.72	993.10	994.9

[a] The energies E_v are measured with respect to the minimum of the PEC.

Table 8. Comparison of Theoretical and Experimental Vibrational Spacings ($E_v - E_{v-1}$) and Rotational Constants for the Ground State of $^{11}B_2$ (Energy unit: cm^{-1})

	$E_v - E_{v-1}$			B_v		
v	theory	experiment	deviation[a]	theory	experiment	deviation[a]
0				1.20639	1.20798[b]	−0.00159
1	1031.93	1032.73[b]	−0.8	1.19202	1.1919[b]	0.00012
2	1014.43			1.17754	1.1789[b]	−0.00136
3	996.72			1.16293		
4	978.80			1.14816		
5	960.64			1.13324		
6	942.22			1.11812		
7	923.52			1.10280		
8	904.53			1.08725		
9	885.22			1.07145		
10	865.57			1.05537		
11	845.56			1.03898		
12	825.15			1.02226	1.00114[c]	0.02112
13	804.32	803.0[c]	1.3	1.00518	0.98562[c]	0.01956
14	783.04	787.0[c]	−3.9	0.98768	0.97502[c]	0.01266
15	761.27	773.0[c]	−11.7	0.96974	0.96111[c]	0.00863

[a] Deviation = theory − experiment. [b] Experimental data of Bredohl et al.[60] [c] Experimental data of Bredohl et al.[61]

$1^3\Sigma_u^-$, and $2^3\Sigma_u^-$. They are listed in Tables S8−S10 of the Supporting Information.

5. INFERENCES FROM COMPARING AB INITIO AND EXPERIMENTAL SPECTROSCOPIC RESULTS

5.1. Spacings of Adjacent Vibrational Levels. The vibrational level spacings ($E_v - E_{v-1}$) predicted by the ab initio calculation are compared with the values deduced from experiment in columns 2−4 of Table 8. The rotational constants B_v are compared in columns 5−7. The vibrational transition ($E_1 - E_0$) of

Table 9. Experimental Electronic Transition Energies of the $^{11}B_2$ Molecule Observed in Emission by Bredohl et al.

assumed transition: $2^3\Sigma_u^-(v'=0) \rightarrow X\ ^3\Sigma_g^-(v)$	
v	observed transition energies
Bredohl et al.[60]	
0	30518.45
1	29485.72
Bredohl et al.[61]	
12	19007
13	18204
14	17417
15	16644
16	15890[a]

[a] This value was dropped from consideration by Bredohl et al.[61] as being too weak for reliable analysis.

Table 10. Comparison of the ab Initio Values of $[E_v - E_0]$ of the $^{11}B_2$ Ground State with the Values Deduced from the Experimental Data in Table 9 under the Assumption, Indicated in That Table, That All Transitions Originate from the Same $2^3\Sigma_u^-(v'=0)$ Level (Energy Unit: cm^{-1})

v	experiment[a]	theory[b]	deviation[c]
1	1032.73	1031.93	0.8
12	11511[d]	11174	337
13	12314[d]	11979	335
14	13101[d]	12762	339
15	13874[d]	13523	351

[a] Values obtained by subtracting the $[2^3\Sigma_u^-(0) \rightarrow X^3\Sigma_g^-(v)]$ transition energies from the $[2^3\Sigma_u^-(0) \rightarrow X^3\Sigma_g^-(0)]$ transition energy, all as listed in Table 9. [b] See Table 5. [c] Experiment − theory. [d] Based on the assumption, indicated in Table 9, that the transitions measured in 1987 originated from the same $2^3\Sigma_u^-(v=0)$ level as those measured in 1982.

Bredohl and co-workers[60] is theoretically reproduced with spectroscopic accuracy (0.8 cm^{-1} error). For the vibrational transitions $\Delta v = 12 \rightarrow 13$, $13 \rightarrow 14$, $14 \rightarrow 15$ deduced by Bredohl et al.[61] the deviations are slightly larger.

5.2. Position of the Level Set $v = 12-15$ Relative to the Lowest Levels. Serious discrepancies were, however, found with respect to the *total* vibrational energies of levels $v = 12-15$. The experimental data reported by Bredohl et al.[60,61] are reproduced in Table 9. As the heading of the columns in this table implies, both sets of transition energies, that for $v = 0$, 1 and that for $v = 12-15$ were presumed to originate from the *same* upper level, namely $2^3\Sigma_u^-(v'=0)$. Under this premise, one readily deduces from this table the energy differences $[E(v) - E(v=0)]$ for the ground state. These are listed in Table 10 in the second column. The third column of this table lists the corresponding theoretical values obtained from the highly accurate ground state PEC calculated in section 2. The deviations listed in the fourth column show that, whereas there is excellent agreement between theory and experiment for $v = 1$, the theoretical levels $v = 12-15$ all lie about 340 cm^{-1} below the experimentally deduced levels! This discrepancy is more than an order of magnitude larger than what, according to all past experiences, is characteristic for ab initio PECs of the quality obtained here. Ab initio potential energy

dx.doi.org/10.1021/jp210473e | J. Phys. Chem. A 2012, 116, 1717–1729

Table 11. Near Degeneracy between Higher Vibrational Levels of the State $1^3\Sigma_u^-$ and Low Vibrational Levels of the State $2^3\Sigma_u^-$ for the B_2 Potentials Displayed in Figure 1 (Near-FCI/cc-pVTZ Level of Theory)[a] (Energy unit: cm^{-1})

$1^3\Sigma_u^-(v'')$		$2^3\Sigma_u^-(v')$	
v	E_v	v	E_v
		0	17116
		1	18036
		2	18954
15	15555		
16	16354		
17	17131		
18	17886		
19	18621		

[a] All energies are measured with respect to the minimum of the $1^3\Sigma_u^-$ potential energy curve.

surfaces determined with this high accuracy typically yield mean absolute errors not exceeding 15 cm^{-1} for the complete set of levels and maximum errors of *at most* ~30 cm^{-1} for individual levels representing the majority of vibrational states, excepting, perhaps, the very highest-lying vibrational levels that are very close to the dissociation limit.

In view of the unlikelihood of a theoretical error of this magnitude, one should recall that only for the levels v = 0, 1 had it been proven[49] that the emission originates from the $2^3\Sigma_u^-(v'=0)$ level. In fact, Hachey, Karna, and Grein[54] had suggested on theoretical grounds that the emission spectrum to the v = 12−15 ground state levels may *not* originate from the $2^3\Sigma_u^-(v'=0)$ level, but instead from highly excited vibrational levels of the $1^3\Sigma_u^-$ electronic state that may gain some population by being near-degenerate with the $2^3\Sigma_u^-(v'=0)$ level. To Hachey et al.,[54] this origin seemed more likely than the possibility that the Franck−Condon factor from the same level, viz. $2^3\Sigma_u^-(v'=0)$, would essentially vanish for the ground state levels v = 3−11 and then surge again for the levels 12−15.

It was to explore these questions that the calculations of the excited potential energy curves were made that were reported above in section 3. The following deductions and calculations are thus based on the (valence near-FCI/cc-pVTZ) level calculations for the three states $X\,^3\Sigma_g^-$, $1^3\Sigma_u^-$, $2^3\Sigma_u^-$ that were discussed in section 3 and whose plots were displayed in Figure 1.

The first question to be answered is, which vibrational levels of the $1^3\Sigma_u^-$ state are near-degenerate with the v' = 0 level of the $2^3\Sigma_u^-$ state? Quantitative information regarding the positions of the spectra of these PECs relative to each other on the energy scale is obtained by combining the values given for E(20 Å) at end of Tables S2, S4, and S6 with the values given for V(eq) and the vibrational levels in Tables S8, S9, and S10 of the Supporting Information. From these tables one deduces the data in Table 11, which show that the levels for v'' = 15−19 of the $1^3\Sigma_u^-$ state fall in the range of $2^3\Sigma_u^-(v'=0)$. The energies of all levels listed in this table are measured with respect to the minimum of the potential energy curve of the $1^3\Sigma_u^-$ state.

The next question is then whether emissions from levels in this range can have sufficient intensity to be observed. The *electronic strengths* of the possible transitions are determined by the transition dipole moments. The magnitudes of transition dipole moments for $1^3\Sigma_u^- \rightarrow X^3\Sigma_g^-$ and $2^3\Sigma_u^- \rightarrow X^3\Sigma_g^-$ transitions in the relevant range of the internuclear distance are listed in Table 12. These transition dipole moments were calculated with the cc-pVTZ based state-averaged CASSCF[6/8] wave functions. The comparison of the energies obtained from these wave functions, which are listed in Table S11 of the Supporting Information, with the potential energy curves obtained from the cc-pVTZ based FCI-CEEIS wave functions, which are displayed in Figures S1 and S2 of the Supporting Information, shows that, for the transition dipole moments, the CASSCF calculation yields a reasonable approximation to the near-FCI calculations. It is apparent that the transition dipole moments for $1^3\Sigma_u^- \rightarrow X^3\Sigma_g^-$, although somewhat smaller than those for $2^3\Sigma_u^- \rightarrow X^3\Sigma_g^-$, are quite significant.

Table 12. Magnitudes of Calculated Transition Dipole Moments (in Atomic Units) for Transitions between the $X\,^3\Sigma_g^-$ Ground State of B_2 and the Excited States $1^3\Sigma_u^-$ and $2^3\Sigma_u^-$[a]

R, Å	$X\,^3\Sigma_g^- \rightarrow 1\,^3\Sigma_u^-$	$X\,^3\Sigma_g^- \rightarrow 2\,^3\Sigma_u^-$
1.30	0.137250	0.717866
1.40	0.126774	0.677706
1.50	0.111986	0.594488
1.60	0.097165	0.472838
1.70	0.087498	0.325946
1.80	0.088956	0.169880
1.90	0.106518	0.018762
2.00	0.140805	0.115977
2.20	0.232850	0.295125
2.30	0.271124	0.321994
2.50	0.299161	0.262372

[a] Orbitals generated by a state-averaged CASSCF[6/8] calculation including the five lowest states of A_u symmetry in D_{2h} with M_S = 1.

The *vibrational strengths* of the transitions are determined by the Franck−Condon (FC) factors. These factors were calculated with the with the vibrational wave functions based on the FCI-CEEIS PECs obtained using the cc-pVTZ basis set (e.g., see Figures S1 and S2 of the Supporting Information which display the vibrational wave functions for v = 0 states of $X\,^3\Sigma_g^-$, $1^3\Sigma_u^-$, and $2^3\Sigma_u^-$). The potential energy curves for these electronic states are also exhibited in Figure 1 (see Tables S1−S6 of the Supporting Information). Three sets of Franck−Condon factors were calculated: the first set for the transitions $[2^3\Sigma_u^-(v'=0) \rightarrow X^3\Sigma_g^-(v)]$, the second set for the transitions $[1^3\Sigma_u^-(v'=16) \rightarrow X^3\Sigma_g^-(v)]$, the third set for the transitions $[1^3\Sigma_u^-(v'=17) \rightarrow X^3\Sigma_g^-(v)]$. The results for the first two sets are displayed in Figure 2. On the left side of this figure, the lower portion of the ground state potential energy curve $X\,^3\Sigma_g^-$ is displayed with the vibrational energy levels from v = 0 to v = 17. On the right side of this figure, the Franck−Condon factors of the $[2^3\Sigma_u^-(v'=0) \rightarrow X^3\Sigma_g^-(v)]$ transitions are represented by blue horizontal bars. They manifestly go to zero beyond v = 2 so that *no transitions from* $[2^3\Sigma_u^-(v'=0)$ *to the ground state are expected to be observed for* $v > 2$. On the other hand, the FC factors of the $[1^3\Sigma_u^-(v'=16) \rightarrow X^3\Sigma_g^-(v)]$ transitions, which are represented by red bars, exhibit quite large FC factors for transitions to the levels v = 12 and higher of the ground state and very similar results are also found for the transitions $[1^3\Sigma_u^-(v'=17) \rightarrow X\,^3\Sigma_g^-(v)]$. Quantitative details for these FC factors are given in Tables S12−14 of the Supporting Information.

Tables S12−S14 (Supporting Information) also give estimated energies for the transitions to the ground states.

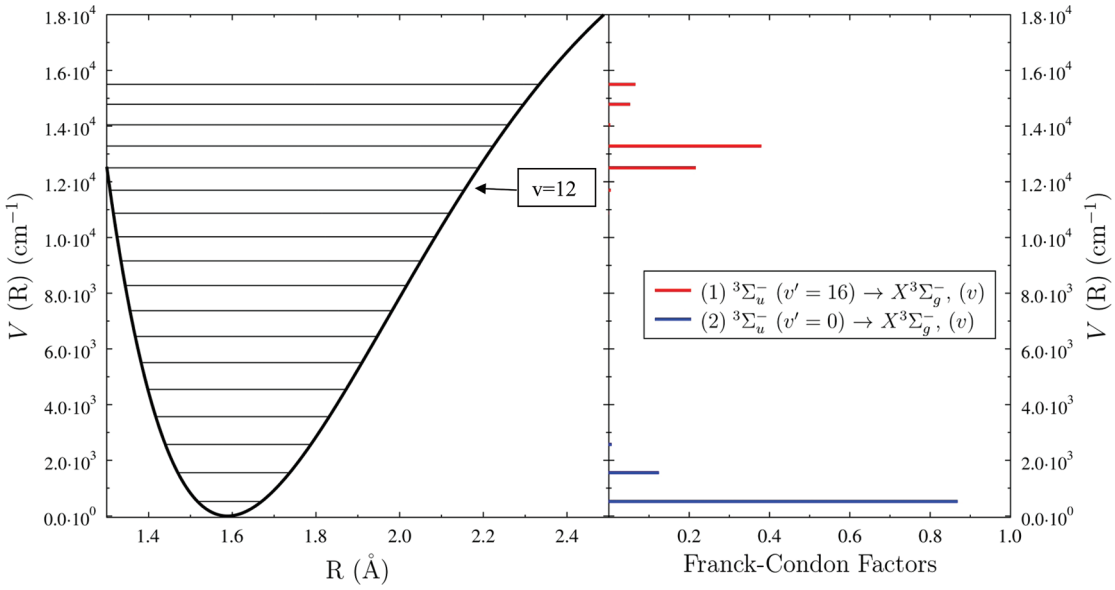

Figure 2. Left panel: lower part of the ground state potential energy curve $X^3\Sigma_g^-$ with the vibrational energy levels from $v = 0$ to $v = 17$. Right panel: Franck−Condon factors calculated for two possible sets of transitions to the ground state vibrational levels: red, originating from the upper state $1^3\Sigma_u^-(v'=16)$; blue, originating from the upper state $2^3\Sigma_u^-(v'=0)$. The Franck−Condon factors are calculated for the potential energy curves displayed in Figure 1.

The *exact* levels and their positions cannot be asserted with certainty because the excited state calculations of section 3 were made at the valence FCI/cc-pVTZ level and neither CBS extrapolation nor core or relativistic corrections were taken into account. The energy levels, which are listed in Tables S8−S10 of the Supporting Information, are quite sensitive to these limitations. Nonetheless, the overall shapes of the excited potential energy curves in Figure 1 are not expected to change very much and the conclusions regarding the Franck−Condon factors are expected to remain valid when the aforementioned refinements are included.

These results make it very likely that the interpretation of Hachey et al.[54] is correct, i.e., that the transitions to the ground state levels $v = 12-15$ originate with the $1^3\Sigma_u^-$ excited state, presumably from levels near $v' = 16$ or 17. It follows that the experimental data for $v = 12-15$ should not be combined with those for $v = 0$ to deduce the energy interval between the levels $v = 12$ and $v = 0$ and that the theoretical interval given in Table 10 is very much closer to the true value.

The combination of the experimental data and the accurate theoretical ground state results that are listed in Table 10 leads then to the conclusion that the pertinent originating level on the $1^3\Sigma_u^-$ state lies about 340 cm^{-1} below the $2^3\Sigma_u^-(v'=0)$ level. The question of the mechanism by which population leaks from the latter to the level on the $1^3\Sigma_u^-$ state transcends the scope of the present inquiry.

6. SUMMARY

As yet, only six vibrational energy levels are known from experiment[60,61] for the $^{11}B_2$ molecule in the ground electronic state, i.e., less than 20% of the total number of vibrational levels obtained in the present study. The theoretical levels were determined from a very accurate ab initio potential energy curve that was calculated as follows:

- An ab initio nonrelativistic valence-electron-correlation-only potential was generated at the near-FCI/complete-basis-set-limit level.
- Core−electron correlation corrections were obtained at the MR-CISD(Q) level of theory with an extrapolation to the complete-basis-set-limit.
- Scalar relativistic corrections were obtained at the CASSCF-[6/8] level of theory with the cc-pVTZ basis set.
- Spin−orbit coupling corrections were obtained at a reduced-full-optimized-reaction-space [2-electrons-in-6-orbitals] level of theory with the cc-pVTZ basis set.

The agreement of the ab initio results with the available experimental data for $^{11}B_2$ is found to be very good for the energy differences between adjacent vibrational levels. For the four known vibrational level spacings, the theory agrees with the experiment within 4.5 cm^{-1} on average.

For the energy differences $[E(v) - E(v=0)]$ with $v = 12-15$, the ab initio results yielded, however, values about 340 cm^{-1} lower than those proposed by the experimentalists who deduced them from their electronic emission spectra. The explanation is very likely that these emissions do not originate from the $v = 0$ level of the $2^3\Sigma_u^-$ state, as assumed by the experimentalists, but rather from certain levels of the $1^3\Sigma_u^-$ state that lie about 340 cm^{-1} lower. This conclusion is based on an ab initio analysis of transition dipoles and Franck−Condon factors.

The dissociation energy D_0 of $^{11}B_2$ is predicted to be 23164 ± 92 cm^{-1}. It agrees with the thermochemical values, which have larger error bars.

It is hoped that the present ab initio analysis will be helpful to further experimental studies of the $^{11}B_2$ and the ^{11}B-^{10}B isotopomers in throwing more light on these systems.

■ ASSOCIATED CONTENT

Supporting Information. Tables documenting the potential energy curves for the ground and excited states. Tables listing vibrational energy levels E_v and rotational constants B_v for the ground and excited states. Tables documenting the Franck−Condon factors corresponding to transitions

from the selected vibrational levels in the excited states $[(2)^3\Sigma_u^-(v''=0)$, $(1)^3\Sigma_u^-(v''=16)$, and $(1)^3\Sigma_u^-(v''=17)]$ to the ground state $X\ ^3\Sigma_g^-(v)$. Tables comparing the theoretical vibrational energy levels with the corresponding levels extracted from the experimental data for $v = 0-14$ of the ground electronic state. Plots displaying vibrational wave functions for $v = 0$ level displayed for the electronic states $X\ ^3\Sigma_g^-$, $1^3\Sigma_u^-$, and $2^3\Sigma_u^-$. This material is available free of charge via the Internet at http://pubs.acs.org.

AUTHOR INFORMATION

Corresponding Author

*E-mail: Laimutis.Bytautas@rice.edu.

ACKNOWLEDGMENT

We thank Professor Robert Le Roy for an extended, instructive, and most helpful exchange notably regarding the rotational spectrum, in particular for kindly providing the authors with the results of the rotational perturbation calculation he obtained using his program LEVEL.[111] His feedback provided the motivation for the quality analysis presented in Table 4. We are grateful to both reviewers for valuable comments and suggestions. We furthermore thank Professor Robert Curl, Professor Fritz Grein, and Mr. Carlos A. Jiménez-Hoyos for useful discussions and valuable suggestions. This work was supported by The Welch Foundation (C-0036). The work was supported by the Division of Chemical Sciences, Office of Basic Energy Sciences, U.S. Department of Energy, under Contract No. DE-AC02-07CH11358 with Iowa State University through the Ames Laboratory.

REFERENCES

(1) Sherrill, C. D. *J. Chem. Phys.* **2010**, *132*, 110902.
(2) Bartlett, R. J. *Chem. Phys. Lett.* **2009**, *484*, 1.
(3) Lodi, L.; Tennyson, J. *J. Phys. B* **2010**, *43*, 133001.
(4) Kowalski, K.; Piecuch, P. *J. Chem. Phys.* **2000**, *113*, 18.
(5) Krylov, A. I. *Chem. Phys. Lett.* **2001**, *350*, 522. Krylov, A. I. *Acc. Chem. Res.* **2006**, *39*, 83–91.
(6) Chan, G. K.-L.; Kállay, M.; Gauss, J. *J. Chem. Phys.* **2004**, *121*, 6110.
(7) Shephard, R.; Minkoff, M. *Int. J. Quantum Chem.* **2006**, *106*, 3190.
(8) Rothman, A. E.; Foley, J. J.; Mazziotti, D. A. *Phys. Rev. A* **2009**, *80*, 052508.
(9) Tsuchimochi, T.; Scuseria, G. E. *J. Chem. Phys.* **2009**, *131*, 121102.
(10) Scuseria, G. E.; Tsuchimochi, T. *J. Chem. Phys.* **2009**, *131*, 164119.
(11) Bytautas, L.; Ruedenberg, K. *J. Phys. Chem. A* **2010**, *114*, 8601.
(12) Bytautas, L.; Henderson, T. M.; Jiménez-Hoyos, C. A.; Ellis, J. K.; Scuseria, G. E. *J. Chem. Phys.* **2011**, *135*, 044119.
(13) Scuseria, G. E.; Jiménez-Hoyos, C. A.; Henderson, T. M.; Samanta, K.; Ellis, J. K. *J. Chem. Phys.* **2011**, *135*, 124108. Jiménez-Hoyos, C. A.; Henderson, T. M.; Scuseria, G. E. *J. Chem. Theory Comput.* **2011**, *7*, 2667–2674.
(14) Booth, G. H.; Cleland, D.; Thom, A. J. W.; Alavi, A. *J. Chem. Phys.* **2011**, *135*, 084104.
(15) Chan, G. K.-L.; Sharma, S. *Annu. Rev. Phys. Chem.* **2011**, *62*, 465.
(16) Chan, G. K.-L. Low entanglement wavefunctions (preprint).
(17) Small, D. W.; Head-Gordon, M. *Phys. Chem. Chem. Phys.* **2011**, *13*, 19285.
(18) Pelzer, K.; Greenman, L.; Gidofalvi, G.; Mazziotti, D. A. *J. Phys. Chem. A* **2011**, *115*, 5632.
(19) Datta, D.; Kong, L. G.; Nooijen, M. *J. Chem. Phys.* **2011**, *134*, 214116.
(20) Jiang, W. Y.; Wilson, A. K. *J. Chem. Phys.* **2011**, *134*, 034101.
(21) Maksyutenko, P.; Rizzo, T. R.; Boyarkin, O. V. *J. Chem. Phys.* **2006**, *125*, 181101.
(22) Heaven, M. C.; Merritt, J. M.; Bondybey, V. E. *Annu. Rev. Phys. Chem.* **2011**, *62*, 375.
(23) Schatz, G. C. *Rev. Mod. Phys.* **1989**, *61*, 669.
(24) Mauguiere, F.; Rey, M.; Tyuterev, V. G.; Suarez, J.; Farantos, S. C. *J. Phys. Chem. A* **2010**, *114*, 9836.
(25) Bowman, J. M.; Braams, B. J.; Carter, S.; Chen, C.; Czakó, G.; Fu, B.; Huang, X.; Kamarchik, E.; Sharma, A. R.; Shepler, B. C.; Wang, Y.; Xie, Z. *J. Phys. Chem. Lett.* **2010**, *1*, 1866.
(26) Dabrowski, I. *Can. J. Phys.* **1984**, *62*, 1639.
(27) Merritt, J. M.; Bondybey, V. E.; Heaven, M. C. *Science* **2009**, *324*, 1548.
(28) Coxon, J. A.; Dickinson, C. S. *J. Chem. Phys.* **2004**, *121*, 9378.
(29) Coxon, J. A.; Molski, M. *Phys. Chem. Comm.* **2004**, *20*, 1.
(30) Colbourn, E. A.; Dagenais, M.; Douglas, A. E.; Raymonda, J. W. *Can. J. Phys.* **1976**, *54*, 1343.
(31) Yang, X.; Wodtke, A. M. *J. Chem. Phys.* **1989**, *90*, 7114.
(32) Jongma, R. T.; Shi, S.; Wodtke, A. M. *J. Chem. Phys.* **1999**, *111*, 2588.
(33) Kolos, W.; Wolnewicz, L. *J. Chem. Phys.* **1964**, *41*, 3663.
(34) Wolniewicz, L. *J. Chem. Phys.* **1995**, *103*, 1792.
(35) Patkowski, K.; Špirko, V.; Szalewicz, K. *Science* **2009**, *326*, 1382.
(36) Szalay, P. G.; Holka, F.; Fremont, J.; Rey, M.; Peterson, K. A.; Tyuterev, V. G. *Phys. Chem. Chem. Phys.* **2011**, *13*, 3654.
(37) Polyansky, O. L.; Császár, A. G.; Shirin, S. V.; Zobov, N. F.; Barletta, P.; Tennyson, J.; Schwenke, D. W.; Knowles, P. J. *Science* **2003**, *299*, 539.
(38) Bytautas, L.; Ruedenberg, K. *J. Chem. Phys.* **2010**, *132*, 074109.
(39) Bytautas, L.; Matsunaga, N.; Ruedenberg, K. *J. Chem. Phys.* **2010**, *132*, 074307.
(40) Bytautas, L.; Ruedenberg, K. *J. Chem. Phys.* **2004**, *121*, 10905.
(41) Bytautas, L.; Ruedenberg, K. *J. Chem. Phys.* **2005**, *122*, 154110.
(42) Bytautas, L.; Ruedenberg, K. *J. Chem. Phys.* **2006**, *124*, 174304.
(43) Bytautas, L.; Nagata, T.; Gordon, M. S.; Ruedenberg, K. *J. Chem. Phys.* **2007**, *127*, 164317.
(44) Bytautas, L.; Matsunaga, N.; Nagata, T.; Gordon, M. S.; Ruedenberg, K. *J. Chem. Phys.* **2007**, *127*, 204301.
(45) Bytautas, L.; Matsunaga, N.; Nagata, T.; Gordon, M. S.; Ruedenberg, K. *J. Chem. Phys.* **2007**, *127*, 204313.
(46) Bytautas, L.; Ruedenberg, K. *J. Chem. Phys.* **2009**, *130*, 204101.
(47) Padgett, A. A.; Griffing, V. *J. Chem. Phys.* **1959**, *30*, 1286.
(48) Bender, C. F.; Davidson, E. R. *J. Chem. Phys.* **1967**, *46*, 3313.
(49) Dupuis, M.; Liu, B. *J. Chem. Phys.* **1978**, *68*, 2902.
(50) Knight, L. B., Jr.; Gregory, B. W.; Cobranchi, S. T.; Feller, D.; Davidson, E. R. *J. Am. Chem. Soc.* **1987**, *109*, 3521.
(51) Pellegati, A.; Marinelli, F.; Roche, M.; Maynau, D.; Malrieu, J. P. *J. Phys. (Paris)* **1987**, *48*, 29.
(52) Carmichael, I. *J. Chem. Phys.* **1989**, *91*, 1072.
(53) Bruna, P. J.; Wright, J. S. *J. Phys. Chem.* **1990**, *94*, 1774.
(54) Hachey, M.; Karna, S. P.; Grein, F. *J. Phys. B* **1992**, *25*, 1119.
(55) Langhoff, S. R.; Bauschlicher, C. W., Jr. *J. Chem. Phys.* **1991**, *95*, 5882.
(56) Peterson, K. A.; Wilson, A. K.; Woon, D. E.; Dunning, T. H., Jr. *Theor. Chem. Acc.* **1997**, *97*, 251.
(57) Müller, T.; Dallos, M.; Lishka, H.; Dubrovay, Z.; Szalay, P. G. *Theor. Chem. Acc.* **2001**, *105*, 227.
(58) Miliordos, E.; Mavridis, A. *J. Chem. Phys.* **2010**, *132*, 164307.
(59) Douglas, A. E.; Herzberg, G. *Can. J. Res. Sect. A* **1940**, *18*, 165.
(60) Bredohl, H.; Dubois, I.; Nzohabonayo, P. *J. Mol. Spectrosc.* **1982**, *93*, 281.
(61) Bredohl, H.; Dubois, I.; Melen, F. *J. Mol. Spectrosc.* **1987**, *121*, 128.
(62) Brazier, C. R.; Carrick, P. G. *J. Chem. Phys.* **1992**, *96*, 8684.
(63) Tam, S.; Macler, M.; DeRosse, M. E.; Fajardo, M. E. *J. Chem. Phys.* **2000**, *113*, 9067.

(64) Dunning, T. H., Jr. *J. Chem. Phys.* **1989**, *90*, 1007.
(65) Schmidt, M. W.; Baldridge, K. K.; Boatz, J. A.; Elbert, S. T.; Gordon, M. S.; Jensen, J. H.; Koseki, S.; Matsunaga, N.; Nguyen, K. A.; Su, S. J.; Windus, T. L.; Dupuis, M.; Montgomery, J. A. *J. Comput. Chem.* **1993**, *14*, 1347.
(66) Werner, H.-J.; Knowles, P. J.; Almlöf, J.; Lindh, R.; Manby, F. R.; Schütz, M.; Celani, P.; Korona, T.; Rauhut, G.; Amos, R. D.; Bernhardsson, A.; Berning, A.; Cooper, D. L.; Deegan, M. J. O.; Dobbyn, A. J.; Eckert, F.; Hampel, C.; Hetzer, G.; Lloyd, A. W.; McNicholas, S. J.; Meyer, W.; Mura, M. E.; Nicklaß, A.; Palmieri, P.; Pitzer, R.; Schumann, U.; Stoll, H.; Stone, A. J.; Tarroni, R.; Thorsteinsson, T. *MOLPRO: a package of ab initio programs.*
(67) Bytautas, L.; Scuseria, G. E.; Ruedenberg, K. *J. Chem. Phys.*, to be submitted.
(68) Ruedenberg, K.; and Sundberg, K. In *Quantum Science*; Calais, J. L., Goscinski, O., Linderberg, J., Öhrn, Y., Eds.; Plenum Publishing Co.: New York, 1976; p 505.
(69) Cheung, L. M.; Sundberg, K. R.; Ruedenberg, K. *Int. J. Quantum Chem.* **1979**, *16*, 1103.
(70) Ruedenberg, K.; Schmidt, M. W.; Gilbert, M. M.; Elbert, S. T. *Chem. Phys.* **1982**, *71*, 41.
(71) Ruedenberg, K.; Schmidt, M. W.; Gilbert, M. M. *Chem. Phys.* **1982**, *71*, 51.
(72) Ruedenberg, K.; Schmidt, M. W.; Gilbert, M. M.; Elbert, S. T. *Chem. Phys.* **1982**, *71*, 65–78.
(73) Roos, B. O. *Adv. Chem. Phys.* **1987**, *69*, 399.
(74) Schmidt, M. W.; Lam, M. T. B.; Elbert, S. T.; Ruedenberg, K. *Theor. Chim. Acta* **1985**, *68*, 69.
(75) Peterson, K. A.; Kendall, R. A.; Dunning, T. H., Jr. *J. Chem. Phys.* **1993**, *99*, 9790.
(76) Yamaguchi, K. *Chem. Phys. Lett.* **1975**, *33*, 330.
(77) Yamaguchi, K.; Ohta, K.; Fueno, T. *Chem. Phys. Lett.* **1977**, *50*, 266.
(78) Pulay, P.; Hamilton, T. P. *J. Chem. Phys.* **1988**, *88*, 4926.
(79) Bofill, J. M.; Pulay, P. *J. Chem. Phys.* **1989**, *90*, 3637.
(80) Bone, R. G. A.; Pulay, P. *Int. J. Quantum Chem.* **1992**, *45*, 133.
(81) Davidson, E. R. *Rev. Mod. Phys.* **1972**, *44*, 451.
(82) Feller, D. *J. Chem. Phys.* **1992**, *96*, 6104.
(83) Feller, D. *J. Chem. Phys.* **1993**, *98*, 7059.
(84) Halkier, A.; Helgaker, T.; Jørgensen, P.; Klopper, W.; Olsen, J. *Chem. Phys. Lett.* **1999**, *302*, 437.
(85) Helgaker, T.; Klopper, W.; Koch, H.; Noga, J. *J. Chem. Phys.* **1997**, *106*, 9639.
(86) Halkier, A.; Helgaker, T.; Jørgensen, P.; Klopper, W.; Koch, H.; Olsen, J.; Wilson, A. K. *Chem. Phys. Lett.* **1998**, *286*, 243.
(87) Werner, H.-J.; Knowles, P. J. *J. Chem. Phys.* **1988**, *89*, 5803.
(88) Langhoff, S. R.; Davidson, E. R. *Int. J. Quantum Chem.* **1974**, *8*, 61.
(89) Woon, D. E.; Dunning, T. H., Jr. *J. Chem. Phys.* **1995**, *103*, 4572.
(90) Douglas, M.; Kroll, N. M. *Ann. Phys. (N. Y.)* **1974**, *82*, 89.
(91) Nakajima, T.; Hirao, K. *Monatsch. Chem.* **2005**, *136*, 965.
(92) Fedorov, D. G.; Nakajima, T.; Hirao, K. *Chem. Phys. Lett.* **2001**, *335*, 183.
(93) de Jong, W. A.; Harrison, R. J.; Dixon, D. A. *J. Chem. Phys.* **2001**, *114*, 48.
(94) Fedorov, D. G.; Gordon, M. S. *J. Chem. Phys.* **2000**, *112*, 5611.
(95) Moore, C. E. *Atomic Energy Levels*; Vol. 1 (Hydrogen trough Vanadium); Circular of the National Bureau of Standards No. 467; U.S. Government Printing Office: Washington, DC, 1949.
(96) Ruedenberg, K.; Raffenetti, R. C.; Bardo, R. D. In *Energy, Structure and Reactivity: Proceedings of the 1972 Boulder Summer Research Conference on Theoretical Chemistry*; Smith, D. W., McRae, W.B., Eds.; Wiley: New York, 1973; p 164.
(97) Schmidt, M. W.; Ruedenberg, K. *J. Chem. Phys.* **1979**, *71*, 3951.
(98) Raffenetti, R. C. *J. Chem. Phys.* **1973**, *59*, 5936–5936.
(99) Le Roy, R. J. In *Molecular Spectroscopy*; Barrow, R. N., Long, D. A., Millen, D. J., Eds.; Specialist Periodical Report 3; Chemical Society: London, 1973; Vol. 1, pp 113−176.
(100) Le Roy, R. J.; Dattani, N. S.; Coxon, J. A.; Ross, A. J.; Crozet, P.; Linton, C. *J. Chem. Phys.* **2009**, *131*, 204309.
(101) Ivanova, M.; Stein, A.; Pashov, A.; Stolyarov, A. V.; Knöckel, H.; Tiemann, E. *J. Chem. Phys.* **2011**, *135*, 174303.
(102) Varandas, A. J. C. *Chem. Phys. Lett.* **2007**, *443*, 398.
(103) Schmidt, M. W.; Ivanic, J.; Ruedenberg, K. *J. Phys. Chem. A* **2010**, *114*, 8687.
(104) Le Roy, R. J. *J. Mol. Spectrosc.* **1998**, *191*, 223.
(105) Verhaegen, G.; Drowart, J. *J. Chem. Phys.* **1962**, *37*, 1367.
(106) Huber, K. P.; Herzberg, G. *Molecular Spectra and Molecular Structure IV. Constants of Diatomic Molecules*; Van Nostrand Reinhold Co.: New York, 1979.
(107) Chase, M. W., Jr.; Davies, C. A.; Downey, J. R., Jr.; Frurip, D. J.; McDonald, R. A.; Syverud, A. N. *J. Phys. Chem. Ref. Data* **1985**, *14*, 1.
(108) Colbert, D. T.; Miller, W. H. *J. Chem. Phys.* **1992**, *96*, 1982.
(109) Hutson, J. *J. Phys. B* **1981**, *14*, 852.
(110) Tellinghuisen, J. *J. Mol. Spectrosc.* **1987**, *122*, 455.
(111) Le Roy, R. J. *Computer code LEVEL 7.5*; University of Waterloo, 2002. See http://scienide2.uwaterloo.ca/~rleroy/level/.